

## Local density of states in double-barrier resonant-tunneling structures. II. Finite-width barriers

J. D. Bruno and T. B. Bahder

*Harry Diamond Laboratories, U. S. Army Laboratory Command, 2800 Powder Mill Road, Adelphi, Maryland 20783-1197*

(Received 11 July 1988; revised manuscript received 26 September 1988)

The local density of states (DOS) in the quantum-well region of a double-barrier resonant-tunneling structure is calculated for the case of zero applied bias. As the barrier potential  $V_0$  goes to zero, the local DOS approaches an  $E^{1/2}$  behavior; as  $V_0$  goes to infinity, a staircaselike local DOS is obtained. A one-dimensional DOS, characterized by a fixed momentum transverse to the barriers, goes like  $E^{-1/2}$  as  $V_0$  goes to zero and like a series of  $\delta$  functions in the limit of infinite  $V_0$ . The behavior of these local-DOS functions is examined for physically realizable structures.

### I. INTRODUCTION

The experimental results of Sollner *et al.*<sup>1</sup> have led to a renewal of interest in the phenomena of resonant tunneling. Epitaxially grown GaAs/Al<sub>x</sub>Ga<sub>1-x</sub>As double-barrier resonant-tunneling (DBRT) structures, similar to those used by Sollner *et al.*, are now the subject of extensive investigation at many laboratories. Growth methods,<sup>2</sup> barrier widths,<sup>3</sup> quantum-well (QW) compositions,<sup>4</sup> spacer-layer widths,<sup>5</sup> etc. are all being varied in order to investigate their impact on resulting device  $I$ - $V$  characteristics. Although a considerable theoretical effort has been devoted to the understanding of transport in these structures, important questions remain unanswered. Principal among these is whether the observed enhancement in current at a particular bias should be attributed to a Fabry-Pérot-like coherence effect,<sup>6</sup> a kinematic effect associated with tunneling from a three-dimensional (3D) to a 2D region (sequential tunneling model),<sup>7</sup> or a combination of both.<sup>8</sup> We believe that careful experiments are needed before these questions are resolved.

In a recent paper,<sup>9</sup> we found the local density of states (DOS) for a model DBRT structure where the double-barrier potentials were represented by  $\delta$  functions. By varying the strength of the  $\delta$ -function potentials in this model, we were able to go continuously from the 3D to the 2D system, and the local DOS evolved from an  $E^{1/2}$  behavior to a staircaselike behavior. The  $\delta$ -function model thus provided a qualitative picture of the crossover from 3D to 2D dynamics. The purpose of this paper is to extend these results to the more realistic case where the barriers are of finite height and thickness and the effective mass changes in passing from the QW region to the barrier regions of the structure.

In the next section, we describe the wave functions for the system and define the DOS functions. We then examine the DOS functions for different parameter sets and

consider the crossover from 3D to 2D behavior. We conclude by presenting an expression for the lifetime of the lowest quasibound state between the barriers in terms of the barrier-region thickness and effective mass.

### II. MODEL AND CALCULATION

In each semiconductor layer comprising a DBRT structure, a one-band effective-mass Hamiltonian can be written in the form

$$H = -\frac{\hbar^2}{2m_c} \nabla^2 + V(z), \quad (1)$$

where  $m_c$  is the conduction-band effective mass characterizing the layer (say,  $m_1$  in the QW region and beyond the barriers, and  $m_2$  in the barrier regions), and the potential  $V(z)$  is given by

$$V(z) = \begin{cases} V_0 & \text{if } a < |z| < a(1+\xi), \\ 0 & \text{otherwise.} \end{cases}$$

In this expression,  $\xi$  is the width of the barriers (in units of  $a$ ) and  $V_0$  is the energy difference between the conduction-band edges in the two different semiconductors. We have solved the reduced equation connected with (1) using the boundary condition  $\psi(\pm L/2) = 0$ , and by requiring that  $\psi$  and  $m_c^{-1} d\psi/dz$  be continuous<sup>10</sup> at  $z = \pm a$  and  $z = \pm a(1+\xi)$ . The normalized even solutions can be written

$$\psi(z) = \frac{F^{1/2}(u)}{\sqrt{L/2}} \phi(z), \quad (2)$$

where  $u \equiv qa$  and  $q$  is the wave-vector component along the  $z$  direction [the energy eigenvalue connected with (1) is given by  $\epsilon_{k,q} = \hbar^2(\mathbf{k}^2 + q^2)/2m_1$  where  $\mathbf{k}$  is the (conserved) two-dimensional wave vector normal to the  $z$  axis]. The function  $\phi(z)$  is expressed in the form

$$\phi(z) = \begin{cases} \cos(uz/a), & |z| \leq a & (3a) \\ d(u) \exp[w(u)z/a] + e(u) \exp[-w(u)z/a], & a \leq |z| \leq a(1+\xi) & (3b) \\ f(u) \exp(iuz/a) + g(u) \exp(-iuz/a), & |z| \geq a(1+\xi) & (3c) \end{cases}$$

where the functions  $d$ ,  $e$ ,  $f$ , and  $g$  can be found in a straightforward manner. The function  $w(u)$  is given by

$$w(u) = \left[ \frac{\tilde{\gamma} - u^2}{\mu} \right]^{1/2}, \quad (4)$$

where  $\mu \equiv m_1/m_2$  and  $\tilde{\gamma}$  is defined by  $\tilde{\gamma} \equiv \gamma - (1-\mu)v^2$ . Here,  $\gamma$  is the dimensionless potential strength given by  $\gamma \equiv 2m_1 V_0 a^2 / \hbar^2$  and  $v \equiv |k|a$ . Finally, the function  $F(u)$  in (2) is given by

$$F(u) = \frac{1}{4|f(u)|^2} = \frac{u^2}{D(u)}, \quad (5)$$

where  $D(u)$  is defined by the expression

$$D(u) = u^2 + \frac{1}{2}[\mu\tilde{\gamma} + (1-\mu)u^2] \left[ \cos^2(u) + \frac{u^2}{\mu(\tilde{\gamma} - u^2)} \sin^2(u) \right] \{ \cosh[2\xi w(u)] - 1 \} \\ - \frac{1}{\mu w(u)} [\mu\tilde{\gamma} + (1-\mu)u^2] u \sin(u) \cos(u) \sinh[2\xi w(u)]. \quad (6)$$

The allowed values for  $u$  in (2) are given by the roots of a transcendental equation. However, in the limit when  $a/L \rightarrow 0$  the root density approaches  $2\pi/L$  and the equation's solution is not necessary. The normalization of the wave functions given above is correct to zeroth order in the ratio  $a/L$ . Also, the odd functions can be obtained from the even ones by making the replacements  $\cos(u) \rightarrow \sin(u)$ , and  $\sin(u) \rightarrow -\cos(u)$  in all functions given above. In what follows, we will distinguish between even and odd solutions with the subscript  $\alpha$  ( $=e,o$ ). When  $\alpha=o$ , the above-mentioned trigonometric replacements are implied.

In order to get some feeling for the nature of the envelope functions given above, we have plotted in Fig. 1(a) the function  $F_e(u)$  versus  $u$  for the case  $v=0, \gamma=2.0, \mu=0.73$ , and  $\xi=1.0$ . This value for  $\gamma$  is not typical of actual DBRT structures. An actual structure would have a larger  $\gamma$ , and its  $F$  function would have much narrower peaks. The peaks in  $F_e$  occur at longitudinal wave vectors for which (even) quasibound states exist in the QW region of the structure. In Fig. 1(b), we plot the squared modulus of the even wave function (for the same parameter set) for two different wave-vector values, one "on resonance" and the other "off resonance." The barrier region is also indicated in the figure, and it is clear that the on-resonance wave function has a substantial amplitude inside the QW region while the off-resonance wave function is depressed.

For more physically relevant parameter sets, the ratio of wave-function amplitudes inside to outside the QW region would be orders of magnitude larger than shown in Fig. 1(b).

Consider now the local DOS at  $\mathbf{r}$  with energy  $E$  defined by

$$N(E, \mathbf{r}) = 2 \sum_{\mathbf{k}, q, \alpha} |\Psi_{\mathbf{k}, q, \alpha}(\mathbf{r})|^2 \delta(E - \varepsilon_{\mathbf{k}, q}). \quad (7)$$

The wave function in (7) is a product of the envelope function and the conduction-band-bottom Bloch function  $u_{c,0}$ . We can define a unit-cell-averaged local DOS by integrating (7) over the volume of the unit cell containing the position  $\mathbf{r}$  and dividing by the cell volume. If one ignores variations in the envelope functions over the in-

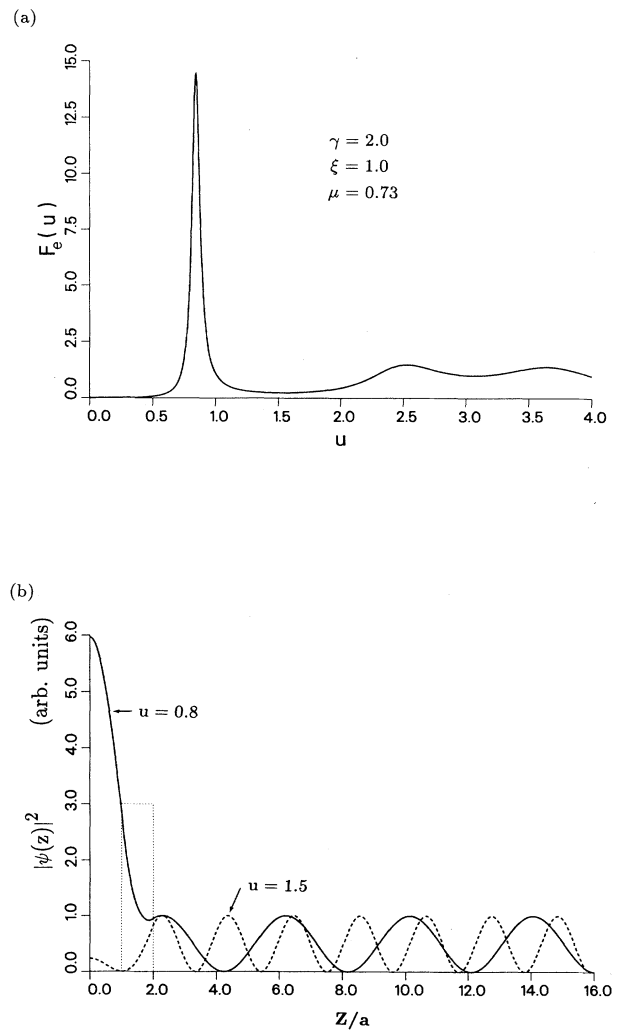


FIG. 1. (a) The function  $F_e(u)$  vs  $u$  for the case  $v=0, \gamma=2.0, \xi=1.0$ , and  $\mu=0.73$ . (b) The squared modulus of two even wave functions vs  $z/a$ . The vertical scale is arbitrary. As is clear from (a), the  $u=0.8$  wave function is "on resonance" and the  $u=1.5$  wave function is "off resonance."

tegration region and takes the Bloch functions to be normalized to unity in a unit cell, one recovers (7) as the unit-cell-averaged local DOS with the wave function interpreted as the envelope function. In what follows, we refer to (7) as the local DOS, understanding that this averaging procedure has been carried out, and interpret the wave functions as envelope functions. To proceed, we replace the wave-vector sums by integrals and define a dimensionless energy  $\varepsilon \equiv 8m_1 a^2 E / \hbar^2 \pi^2$  to obtain

$$N(\varepsilon, z) = \frac{m_1}{\hbar^2 \pi^2 a} \sum_{\alpha} \int_0^{\infty} du \int_0^{\infty} dv^2 |\phi_{\alpha}(u)|^2 F_{\alpha}(u) \times \delta(v^2 - (\pi^2 \varepsilon / 4 - u^2)). \quad (8)$$

$$\bar{N}(\varepsilon) = \frac{m_1}{\hbar^2 \pi^2 a} \int_0^{\pi \sqrt{\varepsilon/2}} du \left[ \frac{1}{2} [F_{e, v_c}(u) + F_{o, v_c}(u)] + \frac{1}{2} [F_{e, v_c}(u) - F_{o, v_c}(u)] \frac{\sin(2u)}{2u} \right], \quad (11)$$

where the subscript  $v_c$  on the  $F$  functions indicates their evaluation at  $v = v_c$ . It is interesting to note that when the effective masses in the QW and barrier regions differ (when  $\mu \neq 1$ ) the contribution to  $\bar{N}(\varepsilon)$  coming from the integrand of (11) at different values of the longitudinal energy component ( $\propto u^2$ ) are contributions one would obtain from different *effective* barrier heights ( $\tilde{\gamma}$ ). This occurs because the  $\delta$  function in the integrand of (8) forces  $\tilde{\gamma}$  to equal  $\gamma - (1 - \mu)(\pi^2 \varepsilon / 4 - u^2)$ . Hence, as  $u$  varies from 0 to its upper limit, the *effective* barrier height increases from a minimum (for  $\mu < 1$ ) of  $\gamma - (1 - \mu)\pi^2 \varepsilon / 4$  to a maximum of  $\gamma$ . At sufficiently high energies, the *effective* barrier height can become negative for much of the integration range. Obviously, any effect this has at high energies (energies much higher than the barrier height) are of academic interest at best since the quadratic dispersion approximation and the one-band approximation break down. However, we find that even at lower energies, in most cases, the effect should not be ignored. We will come back to this point later.

The function  $\bar{N}(\varepsilon)$  provides us with a way of viewing the crossover from a 3D system to a 2D system. In particular, in the limit  $\gamma \rightarrow 0$  (and  $\mu = 1$ ),<sup>11</sup> the functions  $F_e$  and  $F_o$  approach unity and the integral becomes

$$\bar{N}_{\gamma=0}(\varepsilon) = \frac{m_1}{2\hbar^2 \pi a} \sqrt{\varepsilon}, \quad (12)$$

which is the 3D result expected in the absence of barriers. In the opposite extreme, when  $\gamma \rightarrow \infty$ , the integrand approaches a series of  $\delta$  functions at the appropriate bound-state energies of the QW, and the local DOS approaches the form

$$\bar{N}_{\gamma=\infty}(\varepsilon) = \frac{m_1}{2\hbar^2 \pi a} \sum_{n=1}^{\infty} \Theta(\varepsilon - n^2), \quad (13)$$

where  $\Theta$  is the unit step function. This result has the staircaselike appearance characteristic of 2D systems.

The dependence of the envelope function on  $v^2$  is through  $\tilde{\gamma}$ . The  $\delta$  function in the integrand above forces the condition  $v = v_c$ , where  $v_c^2 \equiv \pi^2 \varepsilon / 4 - u^2$ . We then obtain

$$N(\varepsilon, z) = \frac{m_1}{\hbar^2 \pi^2 a} \sum_{\alpha} \int_0^{\pi \sqrt{\varepsilon/2}} du |\phi_{\alpha}(z)|^2 F_{\alpha}(u) \Big|_{v=v_c}. \quad (9)$$

Since we are particularly interested in the average local DOS in the QW region of the structure, we define a spatially averaged local DOS in the QW region by

$$\bar{N}(\varepsilon) = \frac{1}{2a} \int_{-a}^{+a} dz N(\varepsilon, z). \quad (10)$$

With the envelope functions given above,  $\bar{N}(\varepsilon)$  is given by

Finally, one could consider wide barriers with  $\gamma$  held fixed. In this case, the DOS function has a (rounded) staircaselike appearance for energies below the barriers ( $\varepsilon < 4\gamma/\pi^2$ ) and approaches the  $\sqrt{\varepsilon}$  behavior at energies well above the barriers. Analytic approximations for both the height of the steps<sup>12</sup> in the staircaselike structure and their energy positions can be obtained in this case. In Fig. 2, we have plotted  $\bar{N}(\varepsilon)$  versus  $\varepsilon$  for the finite width barrier case  $\gamma = 2.54$ ,  $\xi = 2.0$ , and  $\mu = 0.73$ ; a parameter set appropriate for a typical DBRT structure.<sup>13</sup> We have included in the plot the cases ( $\gamma = 0$ ,  $\mu = 1$ : no barriers) and ( $\gamma = 10^{10}$ ,  $\xi = 10^{-8}$ ,  $\mu = 0.73$ :  $\delta$ -function barriers with large weight),<sup>14</sup> for comparison. Two separate effects, which are partially illustrated by the figure, are worthy of comment. First, on comparing  $\bar{N}(\varepsilon)$  in the no-barrier and large-weight  $\delta$ -function barrier cases, it is evident that the former is larger than the

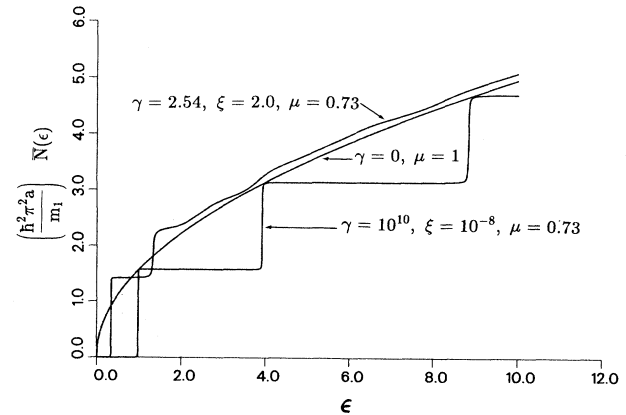


FIG. 2. The local DOS function averaged over the QW region of the structure [ $\bar{N}(\varepsilon)$  vs  $\varepsilon$ ] for the parameter sets shown. In all cases, the transverse wave vector has been set to zero.

latter at all energies, becoming equal only at (sharp) 2D subband edges. When  $\bar{N}(\varepsilon)$  in the finite-width-barrier case is compared to the large-weight  $\delta$ -function case, one can see that the decrease in wave-function localization leads to a substantial downward shift in the lower subband energies and also a smearing out of the lower-subband-edge positions. We find that for parameter sets typical in experimental studies, the downward shift in the energy position of the low-energy subbands is always larger than the corresponding widening of the subband edges. Thus, in general, for finite-width-barrier DBRT structures, the local DOS at the low-energy subband edges is *higher* than the DOS would be at the *same* energies in the absence of barriers. This behavior does not occur in the  $\delta$ -function model. In that case, when the  $\delta$ -function weight is decreased from a large value, the subband-edge widths increase at least as fast as they shift downward in energy and the resulting local DOS remains below the no-barrier ( $\mu=1$ ) DOS function.

Finally, another effect can be seen in the figure that requires explanation. On first examination, it is reasonable to expect that at energies well above the barriers, the DOS for a finite-width barrier structure should approach (and eventually meet) the DOS function for a system without barriers. This assumption is not corroborated by the finite-width barrier  $\bar{N}(\varepsilon)$  case shown in the figure and is generally wrong. The reason the relevant DOS functions do not approach each other is related to the different dispersions (when  $\mu \neq 1$ ) in the barrier and QW regions of the structure. When  $\mu \neq 1$ ,  $\tilde{\gamma}$  becomes a func-

tion of  $u$  in the integrand of (8) as mentioned below (11). Its impact is as follows: at a given value of  $\varepsilon$  and with  $\mu < 1$ ,  $\tilde{\gamma}$  varies from a minimum of  $\gamma - (1-\mu)(\pi^2\varepsilon/4)$  to a maximum of  $\gamma$  as  $u$  varies from 0 to  $\pi\sqrt{\varepsilon}/2$ . At low values of  $u$ , this leads to contributions from the integrand that are characteristic of smaller-barrier systems, i.e., larger contributions than one would obtain if  $\tilde{\gamma}=\gamma$  throughout the range of integration. This results in an increased DOS at all energies above the barriers when compared with the no-barrier (and  $\mu=1$ ) case. When  $\mu > 1$ , the effect is reversed and one finds a lower DOS at high energies than one would obtain in the absence of barriers. This behavior is also seen at energies below the barriers.

It is also instructive to define a 1D local DOS function by fixing the transverse wave vector  $\mathbf{k}$  in (7) and omitting the sum over  $\mathbf{k}$  and the  $L^{-2}$  factor coming from the transverse wave-function normalization. We then define a 1D local DOS by

$$N_{\mathbf{k}}(E_z, z) = 2 \sum_{q, \alpha} |\Psi_{\mathbf{k}, q, \alpha}(z)|^2 \delta(E_z - \varepsilon_{\mathbf{k}, q}). \quad (14)$$

As with (7), we interpret the wave function above to be the envelope function. Again, we replace the sum over  $q$  by an integral and define a dimensionless "z" energy by  $\varepsilon_z \equiv \varepsilon - 4v^2/\pi^2$ . We then integrate (14) over  $z$  from  $-a$  to  $a$  and divide the result by  $2a$ , leading to an expression for the local 1D DOS function averaged over the QW region of the structure:

$$\bar{N}_v(\varepsilon_z) = \frac{2m_1 a}{\hbar^2 \pi} \int_0^\infty du \left[ [F_e(u) + F_o(u)] + [F_e(u) - F_o(u)] \frac{\sin(2u)}{2u} \right] \delta(u^2 - \pi^2 \varepsilon_z / 4). \quad (15)$$

The integral over  $u$  is readily done, and one obtains

$$\bar{N}_v(\varepsilon_z) = \frac{4m_1 a}{\hbar^2 \pi^2} \frac{1}{\sqrt{\varepsilon_z}} \left[ \frac{1}{2} [F_e(u) + F_o(u)] + \frac{1}{2} [F_e(u) - F_o(u)] \frac{\sin(2u)}{2u} \right]_{u=\pi\sqrt{\varepsilon_z}/2}. \quad (16)$$

In the limit  $\gamma \rightarrow 0$  (and  $\mu \rightarrow 1$ ), the term in large parentheses approaches unity, leading to the result

$$\bar{N}_{v, \gamma=0}(\varepsilon_z) = \frac{4m_1 a}{\hbar^2 \pi^2} \frac{1}{\sqrt{\varepsilon_z}}. \quad (17)$$

This agrees with the 1D local DOS one would obtain in the absence of barriers in a 1D problem. In the opposite extreme, when  $\gamma \rightarrow \infty$ , the functions  $F_e$  and  $F_o$  approach sums of  $\delta$  functions with weight  $1/2$ ; each  $\delta$  function corresponds to one of the bound QW states. In this limit, (16) becomes

$$\bar{N}_{v, \gamma=\infty}(\varepsilon_z) = \frac{8m_1 a}{\hbar^2 \pi^2} \sum_{n=1}^{\infty} \delta(\varepsilon_z - n^2). \quad (18)$$

In Fig. 3, we have plotted (16) for the case  $\gamma=2.54$ ,  $\xi=2.0$ , and  $\mu=0.73$ , with  $v=0$  and  $v=\pi/2$ . We have also included the  $\gamma=0$  result for comparison. Note that when  $v$  is increased from zero, the *effective* barrier height

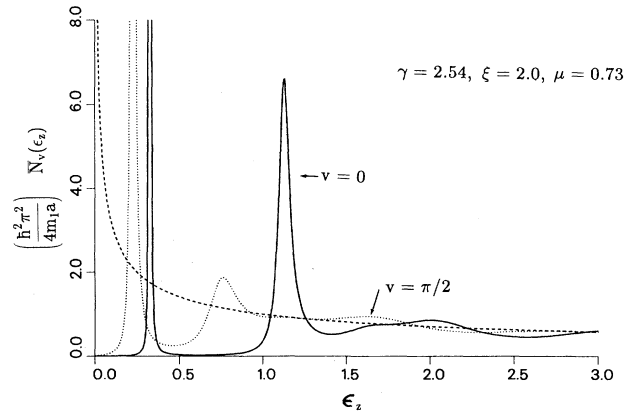


FIG. 3. The local 1D DOS function averaged over the QW region of the structure for the case  $\gamma=2.54$ ,  $\xi=2.0$ , and  $\mu=0.73$ , with  $v=0$  and  $v=\pi/2$ . The latter value of  $v$  corresponds to a transverse kinetic energy  $\varepsilon_1=1$ . The dashed curve shows the  $\gamma=0$ ,  $\mu=1$  case.

decreases; the quasibound states decrease in energy and their widths increase. It is clear from the functional form of  $F_e$  and  $F_o$  that the  $1/\sqrt{\epsilon_z}$  singularity is removed at any finite value of  $\gamma$ , and this is evident in the figure.

### III. CONCLUDING REMARKS

The widths of the peaks in Fig. 3 are inversely proportional to the lifetimes of the corresponding quasibound states in the QW region of the structure. In a recent paper,<sup>15</sup> we showed that each peak in the  $F$  functions corresponded to a complex-conjugate pair of simple poles in  $F$  that led to a Lorentzian form on the real  $u$  axis. We also derived an expression for the lifetime of the lowest-energy quasibound state in terms of the positions of the corresponding poles. In particular, for the lowest quasibound state, we obtained the result

$$\tau = \frac{\pi\tau_0}{32\alpha\beta}, \quad (19)$$

where  $\tau_0 \equiv 16m_1a^2/\pi\hbar$  and  $\alpha+i\beta$  is the position (in the first quadrant of the complex  $u$  plane) of the pole in  $F_e(u)$  with the smallest imaginary part. Since that time, we have learned of the work of Weber *et al.*,<sup>16</sup> who provide an expression for the position of the poles in the limit of large barrier widths (for a structure with a constant effective-mass profile). The strategy described in Ref. 16 uses the fact that for a resonant state whose energy lies below the barriers the wave-function amplitude inside the QW region is substantially larger than the wave function outside the QW region. In the large-barrier limit this will occur only if the coefficient  $d(u)$  in (3), which multiplies the exponentially increasing part of the barrier-region wave function, goes to zero. It is thus natural to search for the zeros of  $f(u)$  [which correspond to the poles of  $F(u)$ ] by expanding the equation  $f(u)=0$  in  $u$  about the point  $u=u_0$  (on the real  $u$  axis) defined as the solution of the transcendental equation

$$\cos(u_0) - \frac{u_0}{\mu w(u_0)} \sin(u_0) = 0, \quad (20)$$

which is equivalent to  $d(u_0)=0$ . When we expand  $f$  about  $u_0$  assuming that  $\exp[-w(u)\xi] \ll 1$  and use the definition  $f(\alpha+i\beta)=0$ , we obtain

$$\alpha+i\beta = u_0 + 2 \exp(-2w_0\xi) \times \exp(2i\phi) \left[ \frac{\mu w_0}{u_0} + \frac{u_0}{\mu w_0} + \frac{1}{u_0} + \frac{u_0}{\mu w_0^2} \right]^{-1}, \quad (21)$$

where  $\tan(\phi) = \mu w_0/u_0$ , and the zero subscripts in (21) indicate evaluation of the various functions at  $u_0$ . This expression can be combined with (19) to give the lifetime of the lowest quasibound state:

$$\tau = \frac{\pi\tau_0}{128u_0} \exp(2w_0\xi) \left[ 1 + \frac{\mu^2 w_0^2}{u_0^2} \right] \times \left[ 1 + \frac{u_0^2}{\mu^2 w_0^2} + \frac{1}{\mu w_0} + \frac{u_0^2}{\mu^2 w_0^3} \right]. \quad (22)$$

When the numerical solution of (20) for  $u_0$  is substituted into (22), the result agrees with earlier numerical work of ours and also (when  $\mu=1$ ) with the work of Weber *et al.*<sup>16</sup>

### ACKNOWLEDGMENTS

The authors take this opportunity to thank C. A. Morrison, J. Sak, B. Sutherland, and D. Wortman for fruitful discussions. We also thank M. Luban and C. L. Hammer for bringing Ref. 16 to our attention.

<sup>1</sup>T. C. L. G. Sollner, W. D. Goodhue, P. E. Tannenwald, C. D. Parker, and D. D. Peck, *Appl. Phys. Lett.* **43**, 588 (1983).

<sup>2</sup>A. R. Bonnefoi, R. T. Collins, T. C. McGill, R. D. Burnham, and F. A. Ponce, *Appl. Phys. Lett.* **46**, 285 (1985).

<sup>3</sup>Masahiro Tsuchiya and Hiroyuki Sakaki, *Jpn. J. Appl. Phys.*, Pt. 2 **25**, L185 (1986).

<sup>4</sup>Hideo Toyoshima, Yuji Ando, Akihiko Okomato, and Tomohiro Itoh, *Jpn. J. Appl. Phys.*, Pt. 2 **25**, L786 (1986).

<sup>5</sup>Shunichi Muto, Tsugano Inata, Hiroaki Ohnishi, Naoki Yokoyama, and Satoshi Hiyamizu, *Jpn. J. Appl. Phys.* **25**, L577 (1986).

<sup>6</sup>R. Tsu and L. Esaki, *Appl. Phys. Lett.* **22**, 562 (1973). See also B. Ricco and M. Ya. Azbel, *Phys. Rev. B* **29**, 29 (1984).

<sup>7</sup>Serge Luryi, *Appl. Phys. Lett.* **47**, 490 (1985).

<sup>8</sup>M. Büttiker, *IBM J. Res. Dev.* **32**, 63 (1988).

<sup>9</sup>T. B. Bahder, J. D. Bruno, R. G. Hay, and C. A. Morrison, *Phys. Rev. B* **37**, 6256 (1988).

<sup>10</sup>The boundary conditions on the slope of  $\psi$ , although conventional, are somewhat arbitrary. Some researchers prefer to

require that the slope of  $\psi$  be continuous.

<sup>11</sup>A physically realizable system would have  $\mu \rightarrow 1$  as  $V_0 \rightarrow 0$ .

<sup>12</sup>One can show that when  $\exp(-w_0\xi) \ll 1$  [where  $w_0 = w(u_0)$  and where  $u_0$  is the real solution to (20)], the weight associated with the sharp  $\delta$ -function-like peaks in  $F$  is given by the expression  $\pi/(1+x)$ , where  $x = (\mu w_0^2 + u_0^2)/(\mu^2 w_0^3 + u_0^2 w_0)$ .

<sup>13</sup>The structure described by Sollner *et al.* in Ref. 1 is characterized by these parameters.

<sup>14</sup>This choice of parameters was made for ease of computation. The results obtained are "near" the  $\gamma = \infty$  case and correspond closely to the  $\delta$ -function barrier model described in Ref. 9 with a  $\delta$ -function potential strength  $U \equiv \gamma\xi = 100$ . Obviously, in the infinite- $\gamma$  case the 2D subband edges would be infinitely sharp.

<sup>15</sup>J. D. Bruno, T. B. Bahder, and C. A. Morrison, *Phys. Rev. B* **37**, 7098 (1988).

<sup>16</sup>T. A. Weber, C. L. Hammer, and V. S. Zidell, *Am. J. Phys.* **50**, 839 (1982).